Marine Ecosystem Model Calibration through Enhanced Surrogate-Based Optimization

Malte Prieß[1], Slawomir Koziel[2], and Thomas Slawig[1]

[1] Institute for Computer Science, Cluster The Future Ocean
Christian-Albrechts Universität zu Kiel, 24098 Kiel, Germany
[2] Engineering Optimization & Modeling Center, School of Science and Engineering
Reykjavik University, Menntavegur 1, 101 Reykjavik, Iceland
{mpr,ts}@informatik.uni-kiel.de, koziel@ru.is

Abstract. Mathematical optimization of models based on simulations usually requires a substantial number of computationally expensive model evaluations and it is therefore often impractical. An improved surrogate-based optimization methodology, which addresses these issues, is developed for the optimization of a representative of the class of one-dimensional marine ecosystem models. Our technique is based upon a multiplicative response correction technique to create a computationally cheap but yet reasonably accurate surrogate from a temporarily coarser discretized physics-based coarse model. The original version of this methodology was capable of yielding about 84% computational cost savings when compared to the fine ecosystem model optimization. Here, we demonstrate that by employing relatively simple modifications, the surrogate model accuracy and the efficiency of the optimization process can be further improved. More specifically, for the considered test case, the optimization cost is reduced three times, i.e., from about 15% to only 5% of the cost of the direct fine model optimization.

Keywords: Marine Ecosystem Models, Surrogate-based Optimization, Parameter Optimization, Response Correction, Data Assimilation.

1 Introduction

Numerical simulations nowadays play an important role to simulate the earth's climate system and to forecast its future behavior. The processes to be modeled and simulated are ranging from fluid mechanics (in atmosphere and oceans) to bio- and biochemical interactions, e.g., in marine or other type of ecosystems. The underlying models are typically given as time-dependent partial differential or differential algebraic equations [7,10,12].

Among them, marine ecosystem models describe photosynthesis and other biogeochemical processes in the marine ecosystem that are important, e.g., to compute and predict the oceanic uptake of carbon dioxide (CO_2) as part of the global carbon cycle [17]. They are typically coupled to ocean circulation models. Since many important processes are non-linear, the numerical effort to simulate the whole or parts of such a coupled system with a satisfying accuracy and resolution is quite high.

N. Pina et al. (Eds.): *Simulation & Modeling Methodologies, Technologies & Appl.*, AISC 197, pp. 193–208.
DOI: 10.1007/978-3-642-34336-0_13

There are processes in the climate system where where even without much simplification (through e.g. "parametrizations" to reduce the system size, see for example [12]) several quantities or parameters are unknown or very difficult to measure. This is for example the case for growth and dying rates in marine ecosystem models [5,17], one of which our work in this paper is based on. Before a transient simulation of a model (e.g., used for predictions) is possible, the latter has to be calibrated, i.e., relevant parameters have to be identified using measurement data (sometimes also known as data assimilation). For this purpose, large-scale optimization methods become crucial for a climate system forecast.

The aim of parameter optimization is to adjust or identify the model parameters such that the model response fits given measurement data. The mathematical task thus can be classified as a least-squares type optimization or inverse problem [2,3,21]. This optimization (or calibration) process requires a substantial number of function and optionally sensitivity or even Hessian matrix evaluations. Evaluation times for the high-fidelity model of several hours, days or even weeks are not uncommon. As a consequence, optimization and control problems are often still beyond the capability of modern numerical algorithms and computer power. For such problems, where the optimization of coupled marine ecosystem models is a representative example, development of faster methods that would reduce the number of expensive simulations necessary to yield a satisfactory solution becomes critical.

Computationally efficient optimization of expensive simulation models (*high-fidelity* or fine models) can be realized using surrogate-based optimization (SBO), see for example [1,6,9,15]. The idea of SBO is to exploit a surrogate, a computationally cheap and yet reasonably accurate representation of the high-fidelity model. The surrogate replaces the original high-fidelity model in the optimization process in the sense of providing predictions of the model optimum. Also, it is updated using the high-fidelity model data accumulated during the process. The prediction-updating scheme is normally iterated in order to refine the search and to locate the high-fidelity model optimum as precisely as possible. One of possible ways of creating the surrogate, our work in this paper is based on, is to utilize a physics-based *low-fidelity* (or coarse) model. The development and use of low-fidelity models obtained by, e.g., coarser discretizations (in time and/or space) or by parametrizations is common in climate research [12], whereas their applications for surrogate-based parameter optimization in this area is new.

In [14], a surrogate-based methodology has been developed for the optimization of climate model parameters. As a case study, a selected representative of the class of one-dimensional marine ecosystem models was considered. Since biochemistry mainly happens locally in space and since the complexity of the biogeochemical processes included in this specific model is high, this model serves as a good test example for the applicability of surrogate-based optimization approaches. The technique described in [14] is based on a multiplicative response correction of a temporally coarser discretized physics-based low-fidelity model. It has been successfully applied and demonstrated to yield substantial computational cost savings of the optimization process when compared to a direct optimization of the high-fidelity model.

In this paper, we demonstrate that by employing simple modifications of the original response correction scheme, one can improve the surrogate's accuracy, as well as further

reduce the computational cost of the optimization process. We verify our approach by using synthetic target data and by comparing the results of SBO with the improved surrogate to those obtained with the original one. The optimization cost is reduced three times when compared to previous results, i.e., from about 15% to only 5% of the cost of the direct high-fidelity ecosystem model optimization (used as a benchmark method). The corresponding time savings are increased to from 84% to 95%.

It should be emphasized that the proposed approach does not rely on high-fidelity model sensitivity data. As a consequence, the first-order consistency condition between the surrogate and the high-fidelity model (i.e., agreement of their derivatives) is not fully satisfied. Nevertheless, the combination of the knowledge about the marine system under consideration embedded in the low-fidelity model and the response correction is sufficient to obtain a quality solution in terms of good model calibration, i.e., its match with the target output.

The paper is organized as follows. The high-fidelity ecosystem model, considered here as a test problem, as well as the low-fidelity counterpart that we use as a basis to construct the surrogate model, are described in Section 2. The optimization problem under consideration is formulated in Section 3. The original and improved response correction schemes and the comparison of the corresponding surrogate model qualities are discussed in Section 4. Numerical results for an illustrative SBO run are provided in Section 5. Section 6 concludes the paper.

2 Model Description

The considered example for the class of one-dimensional marine ecosystem models simulates the interaction of dissolved inorganic nitrogen, phytoplankton, zooplankton and detritus (dead material), thus is of so-called $NPZD$ type [13]. The model uses pre-computed ocean circulation and temperature data from an ocean model (in a sometimes called *off-line mode*), i.e., no feedback by the biogeochemistry on the circulation and temperature is modeled, see again [13]. The original high-fidelity (fine) model and its low-fidelity (coarse) counterpart which we use as a basis to construct a surrogate for further use in the optimization process are briefly described below.

2.1 The High-Fidelity Model

The $NPZD$ model simulates one water column at a given horizontal position. This is motivated by the fact that there have been special time series studies at fixed locations. Clearly, the computational effort in a one-dimensional simulation is significantly smaller than in the three-dimensional case. However, as pointed out in the introduction, the model – from point of view of the complexity of the included processes – serves as a good test example for the applicability of SBO approaches.

In the $NPZD$ model, the concentrations (in mmol N m^{-3}) of dissolved inorganic nitrogen N, phytoplankton P, zooplankton Z, and detritus (i.e., dead material) D are summarized in the vector $y = (y^{(l)})_{l=N,P,Z,D}$ and described by the following coupled PDE system

$$\begin{aligned}
\frac{\partial y^{(l)}}{\partial t} &= \frac{\partial}{\partial z}\left(\kappa \frac{\partial y^{(l)}}{\partial z}\right) + Q^{(l)}(y, u_2, \ldots, u_n), \quad l = N, P, Z, \\
\frac{\partial y^{(D)}}{\partial t} &= \frac{\partial}{\partial z}\left(\kappa \frac{\partial y^{(D)}}{\partial z}\right) + Q^{(D)}(y, u_2, \ldots, u_n) - \frac{\partial y^{(D)}}{\partial z} u_1, \quad l = D,
\end{aligned} \tag{1}$$

in $(-H, 0) \times (0, T)$, with additional appropriate initial values. Here, z denotes the only remaining, vertical spatial coordinate, and H the depth of the water column. The terms $Q^{(l)}$ are the biogeochemical coupling (or *source-minus-sink*) terms for the four tracers and $\mathbf{u} = (u_1, \ldots, u_n)$ is the vector of unknown physical and biological parameters, with $n = 12$ for this specific model. The sinking term (with the sinking velocity u_1) is only apparent in the equation for detritus. In the one-dimensional model no advection term is used, since a reduction to vertical advection would make no sense. Thus, the circulation data (taken from an ocean model) are the turbulent mixing coefficient $\kappa = \kappa(z, t)$ and the temperature $\Theta = \Theta(z, t)$, which goes into the nonlinear coupling terms $Q^{(l)}$ but is omitted in the notation.

The parameters $\mathbf{u}$ to be optimized are, for example, growth and dying rates of the tracers and thus appear in the nonlinear coupling terms $Q^{(l)}_{l=N,P,Z,D}$ in (1). For the sake of brevity and for the purpose of this paper we omit the explicit formulation of the coupling terms as well as the explicit physical meaning of the involved parameter. For details we refer the reader to [13,16].

2.2 Numerical Solution

The continuous model (1) is discretized and solved using an operator splitting method [11], an explicit Euler time stepping scheme for the nonlinear coupling terms Q and the sinking term while using an implicit scheme for the diffusion term. For further details we refer the reader to [13,14].

More explicitly, in every discrete time step, at first the nonlinear coupling operators Q_j (that depend on t_j directly and/or via the temperature field Θ) are computed at every spatial grid point and integrated by four explicit Euler steps with step size $\tau/4$. Then, an explicit Euler step with full step size τ is performed for the sinking term. Finally, an implicit Euler step for the diffusion operator, again with full step size τ, is applied.

In the original model, the time step τ is chosen as one hour. By choosing this time step, all relevant processes are captured and further decrease of the time step does not improve the accuracy of the model. The model with this particular time step will be referred to as the high-fidelity or fine one in the following.

We furthermore denote by $\mathbf{y}_j \approx y(\cdot, t_j)$ the discrete fine model solution of the continuos model (1) in time step j (containing all tracers N, P, Z, D) given as

$$\mathbf{y}_j = (y_{ji})_{i=1,\ldots,I}, \quad j = 1, \ldots, M_f, \quad \mathbf{y} \in \mathbb{R}^{M_f I}, \quad I = n_z n_t, \tag{2}$$

where I denotes the number of spatial discrete points n_z times the number of tracers n_t, which is four for the considered model, and where M_f denotes the total number of discrete time steps, given the discrete time step τ_f. More specifically, the model consists of $n_z = 66$ vertical layers and is integrated over totally $M_f = 8760$ time steps/year $\times$

$5\,\text{years} = 43800$ discrete time step. We will furthermore use the subscript f to distinguish the relevant fine model variables, which read $\mathbf{y}_f, \tau_f$ and M_f, from those we will introduce for the coarse model, respectively.

2.3 The Low-Fidelity Model

Marine ecosystem model, are typically given as coupled time-dependent partial differential equations, compare [5,17]. One straightforward way to introduce a low-fidelity (or coarse) model for these models is to reduce the spatial and/or temporal resolution, whereas, in this paper, we exploit the latter one.

The coarse model, which is a less accurate but computationally cheap representation of $\mathbf{y}_f$ is obtained by using a coarser time discretization with a discrete time step τ_c given as

$$\tau_c = \beta \tau_f, \tag{3}$$

with a *coarsening factor* $\beta \in \mathbb{N} \setminus \{0, 1\}$, while keeping the spatial discretization fixed. The state variable for this coarser discretized model will be denoted by $\mathbf{y}_c$, the corresponding number of discrete time steps by $M_c = M_f/\beta$, i.e., we have

$$(\mathbf{y}_c)_j = ((y_c)_{ji})_{i=1,\ldots,I}, \quad j = 1, \ldots, M_c, \quad \mathbf{y}_c \in \mathbb{R}^{M_c I}, \quad I = n_z n_t\,. \tag{4}$$

Note that the parameters $\mathbf{u}$ for this model are the same as for the fine one.

Clearly, the choice of the temporal discretization, or equivalently, the coarsening factor β, determines the quality of the coarse model and of a surrogate if based upon the latter one. Moreover, both the computational cost, the performance and quality of the solution obtained by a SBO process might be affected.

Altogether, we seek for a reasonable trade-off between the accuracy and speed of the coarse model. From numerical experiments, a value of $\beta = 40$ turned out be a reasonable choice, as was shown in [14]. Numerical results presented in Section 4 demonstrate that such a coarse model leads to a reliable approximation of the original fine ecosystem model when a response correction technique as described in this paper is utilized. Furthermore, it was observed that, for this specific choice of β, while additionally restricting the parameter u_1, i.e., the sinking velocity, using an appropriate upper bound, the resulting model response does not show any numerical instabilities.

3 Optimization Problem

The task of parameter optimization in climate science typically is to minimize a least-squares type cost function measuring the misfit between the discrete model output $\mathbf{y} = \mathbf{y}(\mathbf{u})$ and given observational data $\mathbf{y}_d$ [2,21]. In most cases, the problem is constrained by parameter bounds. The optimization problem can generally be written as

$$\min_{\mathbf{u} \in U_{ad}} \; J(\,\mathbf{y}(\mathbf{u})\,), \tag{5}$$

where

$$\begin{aligned} &J(\,\mathbf{y}\,) := ||\,\mathbf{y} - \mathbf{y}_d\,||^2, \\ &U_{ad} := \{\mathbf{u} \in \mathbb{R}^n : \mathbf{b}_l \le \mathbf{u} \le \mathbf{b}_u\}, \mathbf{b}_l, \mathbf{b}_u \in \mathbb{R}^n,\, \mathbf{b}_l < \mathbf{b}_u\,. \end{aligned} \tag{6}$$

The inequalities in the definition of the set U_{ad} of admissible parameters are meant component-wise. The functional J may additionally include a regularization term for the parameters. However, from numerical experiments, it turned out that such a term is not necessary to ensure a well performing optimization process.

Additional constraints on the state variable $\mathbf{y}$ might be necessary, e.g., to ensure non-negativity of the temperature or of the concentrations of biogeochemical quantities. In our example model, however, by using appropriate parameter bounds $\mathbf{b}_l$ and $\mathbf{b}_u$, non-negativity of the state variables can be ensured. This was already observed and used in [16].

4 Surrogate-Based Optimization

For many nonlinear optimization problems, a high computational cost of evaluating the objective function and its sensitivity, and, in some cases, the lack of sensitivity information, is a major bottleneck. The need for decreasing the computational cost of the optimization process is especially important while handling complex three-dimensional models.

Surrogate-based optimization [1,6,9,15] is a methodology that addresses these issues by replacing the original high-fidelity or fine model $\mathbf{y}$ by a surrogate, in the following denoted by $\mathbf{s}$, a computationally cheap and yet reasonably accurate representation of $\mathbf{y}$.

Surrogates can be created by approximating sampled fine model data (*functional* surrogates). Popular techniques include polynomial regression, kriging, artificial neural networks and support vector regression [15,18,19]. Another possibility, exploited in this work, is to construct the surrogate model through appropriate correction/alignment of a low-fidelity or coarse model (*physics-based* surrogates) [20].

Physics-based surrogates inherit physical characteristics of the original fine model so that only a few fine model data is necessary to ensure their good alignment with the fine model. Moreover, generalization capability of the physics-based models is typically much better than for functional ones. As a results, SBO schemes working with this type of surrogates normally require small number of fine model evaluations to yield a satisfactory solution. On the other hand, their transfer to other applications is less straightforward since the underlying coarse model and chosen correction approach is rather problem specific. The specific correction technique exploited in this work is recalled in Section 4.1 (see also [14]).

The surrogate model is updated at each iteration k of the optimization algorithm, typically using available fine model data from the current and/or also from previous iterates. The next iterate, $\mathbf{u}_{k+1}$, is obtained by optimizing the surrogate $\mathbf{s}_k$, i.e.,

$$\mathbf{u}_{k+1} = \operatorname*{argmin}_{\mathbf{u} \in U_{ad}} J\left(\mathbf{s}_k(\mathbf{u})\right), \tag{7}$$

where, again U_{ad} denotes the set of admissible parameters. The updated surrogate $\mathbf{s}_{k+1}$ is determined by re-aligning the coarse model at $\mathbf{u}_{k+1}$ and optimized again as in (7). The process of aligning the coarse model to obtain the surrogate and subsequent optimization of this surrogate is repeated until a user-defined termination condition is satisfied, which can be based on certain convergence criteria, assumed level of cost function

value or a specific number of iterations (particularly if the computational budget of the optimization process is limited).

If the surrogate $\mathbf{s}_k$ satisfies so-called zero-order and first-order consistency conditions with the fine model at $\mathbf{u}_k$, i.e.,

$$\mathbf{s}_k(\mathbf{u}_k) = \mathbf{y}_f(\mathbf{u}_k), \quad \mathbf{s}'_k(\mathbf{u}_k) = \mathbf{y}'_f(\mathbf{u}_k), \tag{8}$$

with $\mathbf{y}'$ and $\mathbf{s}'_k(\mathbf{u}_k)$ denote the derivatives of the responses, the surrogate-based scheme (7) is provable convergent to at least a local optimum of (5) under mild conditions regarding the coarse and fine model smoothness, and provided that the surrogate optimization scheme (7) is enhanced by the trust-region (TR) safeguard, i.e.,

$$\mathbf{u}_{k+1} = \underset{\substack{\mathbf{u}\in U_{ad},\\ \|\,\mathbf{u}-\mathbf{u}_k\,\| \le \delta_k}}{\operatorname{argmin}} J\,(\,\mathbf{s}_k(\mathbf{u})\,), \tag{9}$$

with δ_k being the trust-region radius updated according to the TR rules. We refer the reader to e.g. [4,8] for more details.

4.1 Surrogate Model Using Basic Multiplicative Response Correction

It has been found in [14] that a natural way of constructing the surrogate would be *multiplicative response correction*. This approach is motivated by the fact that the qualitative relation of the fine and coarse model response is rather well preserved (at least locally) while moving from one parameter vector to another. As a result, a multiplicative correction allows constructing a surrogate model with a good generalization capability. The technique is briefly recalled below.

The surrogate response $\mathbf{s}_k(\mathbf{u})$, at iteration *k* of the optimization process, is generated by multiplicative correction of the *smoothed* coarse model response, denoted by $\tilde{\mathbf{y}}_c$, which we briefly formulate as

$$\left.\begin{aligned} \bar{\mathbf{s}}_k(\mathbf{u}) &:= \mathbf{a}_k\,\tilde{\mathbf{y}}_c(\mathbf{u}), \\ \mathbf{a}_k &:= \frac{\tilde{\mathbf{y}}_f^{\beta}(\mathbf{u}_k)}{\tilde{\mathbf{y}}_c(\mathbf{u}_k)} \end{aligned}\right\} \quad \begin{aligned} &k = 1, 2, \ldots \\ &\beta = M_f/M_c \end{aligned} \tag{10}$$

where the operations in (10) are meant point-wise and where a_k denote the *correction factors* which are included in the vector $\mathbf{a}_k$. They are defined as the point-wise division of the smoothed and *down-sampled* fine model response, denoted by $\tilde{\mathbf{y}}_f^{\beta}$, by the smoothed coarse model response at the point $\mathbf{u}_k$.

It was observed that smoothing allows us to remove the numerical noise from the coarse model response and identify the main characteristics of the traces of interest (see [14] for details). The fine model response is smoothed accordingly in the formulation (10).

Down-sampling was necessary to make the fine model response commensurable with the corresponding response of the coarse model. The down-sampled fine model response $\mathbf{y}_f^{\beta}$ is simply given as

$$y_{ji}^{\beta} := y_{\beta j,i}, \quad j = 1, \ldots, M_c, \quad i = 1, \ldots, I\,. \tag{11}$$

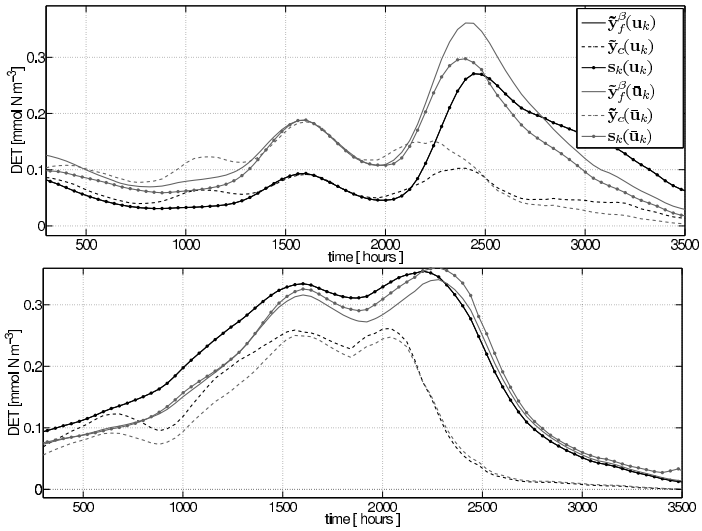

Fig. 1. Surrogate's, fine (down-sampled, smoothed) and coarse (smoothed) model responses $\mathbf{s}_k, \tilde{\mathbf{y}}_f^{\beta}$ and $\tilde{\mathbf{y}}_c$ for the tracer detritus at the uppermost depth layer at two points $\mathbf{u}_k$ and corresponding perturbation $\bar{\mathbf{u}}_k$, illustrating the generalization capability of the surrogate

By definition, the surrogate model is zero-order consistent with the (down-sampled and smoothed) fine model in the point $\mathbf{u}_k$, i.e.,

$$\mathbf{s}_k(\mathbf{u}_k) = \tilde{\mathbf{y}}_f^{\beta}(\mathbf{u}_k)\,. \tag{12}$$

As we do not use sensitivity information from the fine model, the first-order consistency condition cannot be satisfied exactly. Nevertheless, as was shown in [14], this surrogate model exhibits quite good generalization capability, which means that the surrogate provides a reasonable approximation of the fine one in the neighborhood of $\mathbf{u}_k$.

Figure 1 shows the surrogate's, fine (down-sampled) and coarse model responses $\mathbf{s}_k, \tilde{\mathbf{y}}_f^{\beta}$ and $\tilde{\mathbf{y}}_c$ at two different points, $\mathbf{u}_k$ and $\bar{\mathbf{u}}_k$. The surrogate model is established at $\mathbf{u}_k$ and, therefore, its response is perfectly aligned with the one of the fine model at $\mathbf{u}_k$, whereas its prediction is still reasonably accurate at $\bar{\mathbf{u}}_k$.

Note that only the selected tracers for a chosen section in the whole time interval and at one selected depth layer are shown. The total dimension of the model response is too large to present a full response here. We emphasize that shown responses are representative for the overall qualitative behavior the other tracers, time sections and depth layers.

4.2 Difficulties of Basic Surrogate Formulation

Occasionally, when using the surrogate given in (10), there might occur a situation where the coarse model response is close to zero (and maybe even negative due to approximation errors) and a few magnitudes smaller than the fine one, which leads to

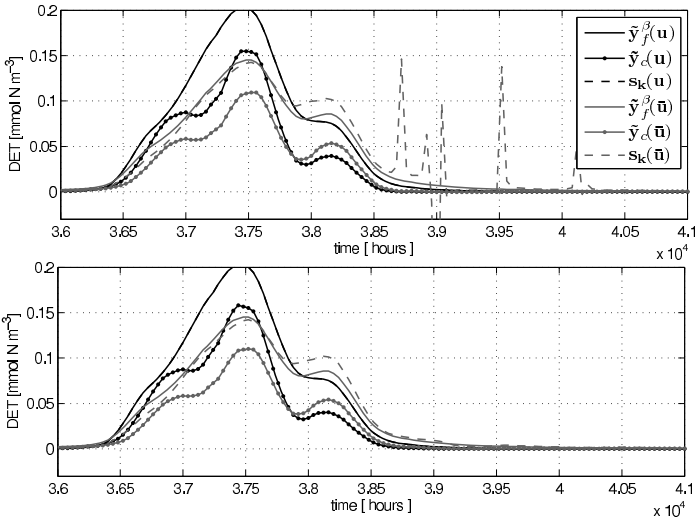

Fig. 2. Responses as in Figure 1 for a different time interval using the basic surrogate formulation (10) (top) and exploiting the modifications (13) of the response correction scheme (bottom)

large (possibly negative) correction factors a_k. While such a correction ensures zero-order consistency at the point where it was established (i.e., $\mathbf{u}_k$), it may lead to (locally) poor approximation in the vicinity of $\mathbf{u}_k$.

Figures 2 and 3 (top) illustrate these issues by showing the smoothed surrogate's, fine (down-sampled) and coarse model responses $\mathbf{s}_k, \tilde{\mathbf{y}}_f^{\beta}$ and $\tilde{\mathbf{y}_c}$ for the state detritus at one illustrative time interval and depth layer. Shown are the model responses at the same points $\mathbf{u}_k$ and its neighborhood $\bar{\mathbf{u}}_k \in B_\delta(\mathbf{u}_k)$ as in Figure 1.

It should be pointed out that the overall shape of the surrogate's response still provides a reasonable approximation of the fine model one (and more accurate than the corresponding coarse model response) despite of the distortion illustrated in Figures 2 and 3. This is supported by the fact that even without addressing these issues, the SBO was able to yield satisfactory results, not only with respect to the quality of the final solution, but, most importantly, in terms of the low computational cost of the optimization process. This was already demonstrated in [14].

4.3 Improved Response Correction Scheme

The response distortion described in the previous section is problematic towards the end of the surrogate-based optimization run when a higher accuracy of the surrogate is required to locate the fine model optimum more accurately. The "'spikes"' appearing in the response due to large values of the correction term can be viewed, in a way, as a numerical noise that slows down the algorithm convergence and makes the optimum more difficult to locate.

A few simple means described below can address these issues and further improve the accuracy of the surrogate's response as well as the performance of the optimization algorithm. We introduce non-negative bounds for the coarse model response (the

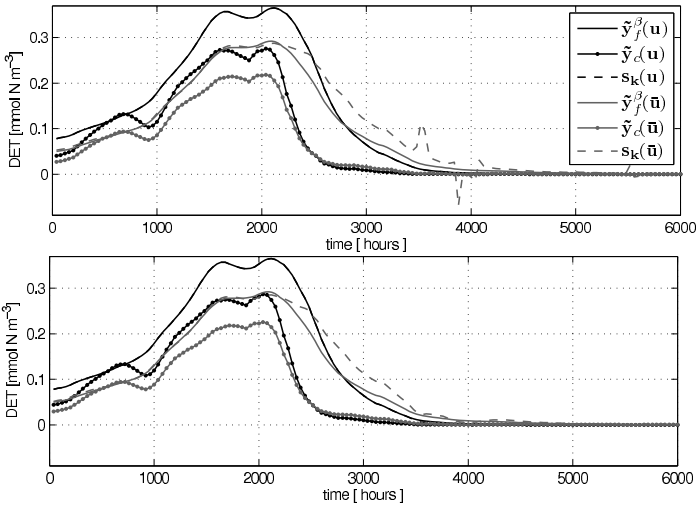

Fig. 3. Responses as in Figure 2, but for yet another section within the whole time interval. Again, after employing the improvements in (13), the positive and negative peaks are removed (bottom).

negative response is non-physical and is a result of numerical errors due to using large time steps in the numerical solution of the coarse model) and an upper bound a_{ub} for the correction factors. We furthermore restrict the correction factors to one in case the fine and coarse model responses are below a certain threshold ϵ which should be of the order of the discretization error below which the responses can be treated as zero.

More specifically, the following modifications of the model outputs and the scaling factors are performed for each iteration k

$$(i)\ \mathbf{y}_c = \begin{cases} 0; & \text{if } \mathbf{y}_c \le 0 \\ \mathbf{y}_c; & \text{else} \end{cases}, \quad (ii)\ \mathbf{a}_k = \begin{cases} a_{\text{ub}}; & \text{if } \mathbf{a}_k \ge a_{\text{ub}} \\ \mathbf{a}_k; & \text{else} \end{cases}, \tag{13}$$

$$(iii)\ \mathbf{a}_k = 1 \text{ if } (\tilde{\mathbf{y}}_f^{\beta} \le \epsilon \text{ and } \tilde{\mathbf{y}}_c \le \epsilon),$$

where the operations are again meant point-wise and where (i) is applied before smoothing. From numerical experiments, $a_{\text{ub}} = 10$ turned out to be a reasonable choice and we furthermore consider $\epsilon = 10^{-4}$.

Figure 2 (bottom) shows the surrogate's, fine (down-sampled) and coarse model response for the same illustrative tracer, time interval and depth layer, however, while employing the improvements given in (13). It can be observed that the positive and negative peaks present in the surrogate responses shown in Figure 2 (top) are removed after applying (13). As additional evidence, Figure 3 (bottom) shows the same model responses but for a different section within the whole time interval.

The numerical results presented in Section 5 demonstrate that this enhanced response correction scheme allows us to further improve the computational efficiency of the SBO.

5 Numerical Results

For all optimization runs, we use the MATLAB[1] function `fmincon`, exploiting the active-set algorithm. The following cost functions

$$J(\mathbf{z}) := \| \mathbf{z} - \mathbf{y}_d \|^2 = \sum_{i=1}^{I} \sum_{j=1}^{M_c} \left(z_{ji} - (y_d)_{ji} \right)^2 , \tag{14}$$

$$\tilde{J}(\mathbf{z}) := \| \mathbf{z} - \tilde{\mathbf{y}}_d \|^2 = \sum_{i=1}^{I} \sum_{j=1}^{M_c} \left(z_{ji} - (\tilde{y}_d)_{ji} \right)^2 , \tag{15}$$

were the target data – as a test case – is given by model generated, attainable data as

$$\mathbf{y}_d := \mathbf{y}_f^{\beta}(\mathbf{u}_d) .$$

For the optimization runs presented in this paper we employ the following cost functions: for the fine model optimization, we use (14) with $\mathbf{z} = \mathbf{y}_f^{\beta}$, for the coarse model optimization, (15) with $\mathbf{z} = \tilde{\mathbf{y}}_c$ and for the SBO, (15) with $\mathbf{z} = \mathbf{s}_k$, whereas (14) was used in the termination condition and to compare the results and where the down-sampled fine model response $\mathbf{y}_f^{\beta}$ is defined by (11). Sampling was necessary to yield a comparable fine model optimization run while in (15) the smoothed target data is considered accordingly, since the coarse model and thus also the surrogate's response are smoothed. Note that the cost functions we employ are not normalized by the total number of discrete model points. The dimension of the responses is of the order of 10^5. Clearly, this has to be taken into account for presented cost function values in the following.

We perform an exemplary direct fine and coarse model optimization as well as a SBO based on the surrogate in (10) exploiting the original and improved response correction scheme (cf. Sections 4.1, 4.3). In the following, the solutions of the four optimization runs are compared through visual inspection of the (down-sampled) fine model response $\mathbf{y}_f^{\beta}$ and the corresponding cost function value $J(\mathbf{y}_f^{\beta})$ (cf. (14)) at the respective optima.

The optimization cost is measured in *equivalent* fine model evaluations which are determined taking into account the coarsening factor β. More specifically, one evaluation of the coarse model with a coarsening factor β is equivalent to $1/\beta$ evaluations of the fine model. On the other hand, the cost of one iteration of the SBO (in terms of equivalent fine model evaluations) equals to the number of coarse model evaluations necessary to optimize the surrogate model divided by this factor β, and increased by the cost for the response correction. Recall that the specific correction (10) we use in this paper requires one fine model evaluation only.

Figure 4 shows the value of the cost function $J(\mathbf{y}_f^{\beta})$ versus the equivalent number of fine model evaluations for the SBO algorithm using the surrogate model exploiting the original and the improved correction scheme, as well as for the fine and coarse model optimization. Points 1 and 3 in Figure 4 indicate those solutions obtained in the SBO

[1] MATLAB is a registered trademark of The MathWorks, Inc., `http://www.mathworks.com`

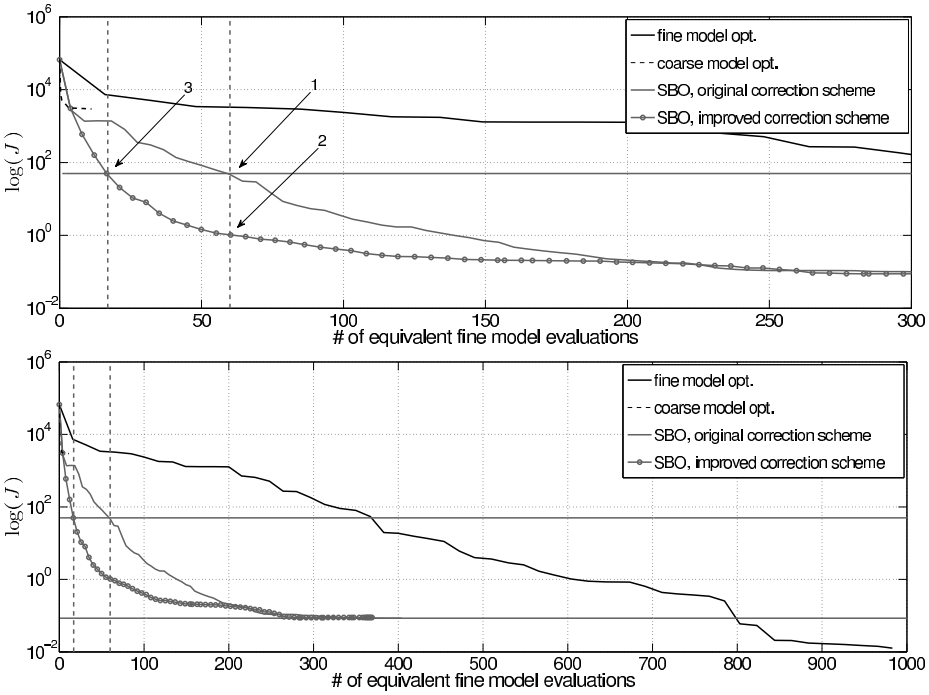

Fig. 4. Values of the cost function J versus the optimization cost measured in *equivalent number* of fine model evaluations for an exemplary SBO run exploiting the original and the improved correction scheme, as well as for a fine and coarse model optimization run. Points 1 and 3 correspond to a termination condition of $J \leq 50$ (upper horizontal line), ensuring good visual agreement between the fine model output and the target. Solution at point 2 in the improved SBO is significantly more accurate and obtained at the same cost as the one at point 1. Overall, SBO converges to a cost function value of to $J \approx 10^{-1}$ (lower horizontal line).

runs that correspond to a termination condition of $J \leq 50$. This particular value was selected as it ensures good visual agreement between the fine model output and the target. Point 2 denotes the solution in the improved SBO run which could be obtained at the same optimization cost as the one at point 1 in the original SBO run.

Figure 5 shows the fine model response at the solutions $\mathbf{u}_{s1}^*$ and $\mathbf{u}_{s2}^*$ (corresponding to points 1 and 2 in Figure 4) obtained using the SBO algorithm with the original and improved response correction scheme (cf. Sections 4.1 and 4.3) as well the responses at the solutions $\mathbf{u}_f^*, \mathbf{u}_c^*$ of a direct fine and coarse model optimization. For illustration, responses for two representative tracers and for a selected depth level and time interval are shown. Corresponding parameter values are provided in Table 1.

It can be observed that coarse model optimization yields a solution far away from the target and a rather inaccurate parameter match (cf. Table 1), whereas the optimization cost of only 11 equivalent fine model evaluations is very low. However, results indicate that the accuracy of the coarse model is not sufficient to use this very model directly in an optimization.

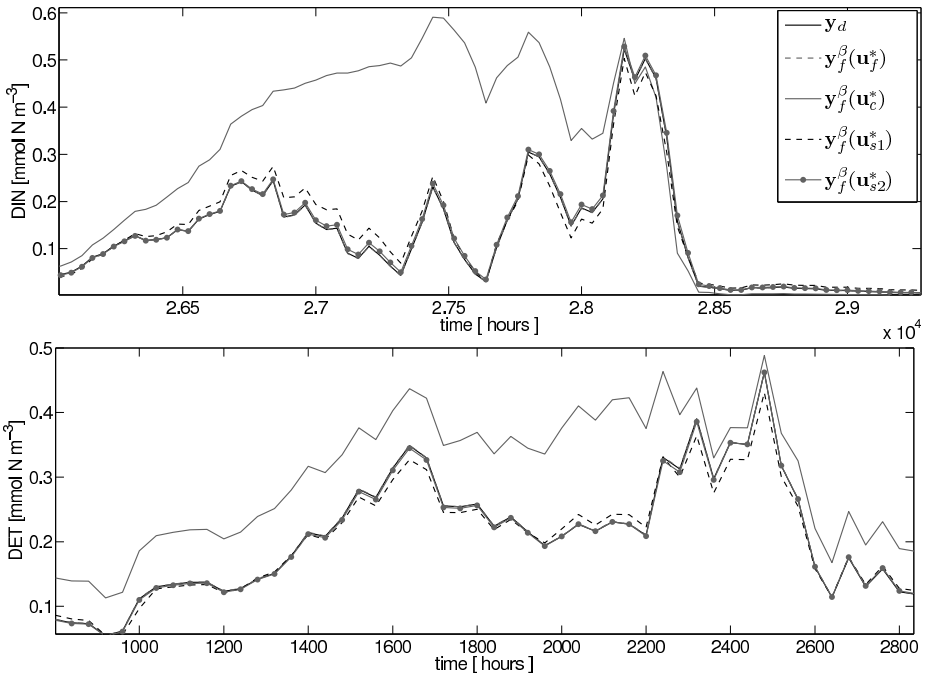

Fig. 5. Synthetic target data $\mathbf{y}_d$ at optimal parameters $\mathbf{u}_d$ and fine model response $\mathbf{y}_f^\beta$ (down-sampled) for two illustrative tracers and at the uppermost depth layer for the solutions $\mathbf{u}_f^*$, $\mathbf{u}_c^*$, $\mathbf{u}_{s1}^*$ and $\mathbf{u}_{s2}^*$ of a direct fine and coarse model optimization as well as of a SBO run exploiting the original and the improved correction scheme. Solutions $\mathbf{u}_{s1}^*$ and $\mathbf{u}_{s2}^*$ correspond to points 1 and 2 in Figure 4

On the other hand, direct fine model optimization yields a solution $\mathbf{u}_f^*$ with an almost perfect fit of the target data (cf. Figure 5) and of the optimal parameters $\mathbf{u}_d$ (cf. Table 1), corresponding to a very low cost function of $J \approx \cdot 10^{-2}$. However, the optimization cost is substantially higher: about 980 fine model evaluations.

In [14], we demonstrated that in a exemplary SBO run based on the original response correction scheme, a reasonably accurate solution $\mathbf{u}_{s1}^*$ could be obtained at the cost of approximately 60 equivalent fine model evaluations only (point 1 in Figure 4). This resulted in a significant reduction of the total optimization cost of about 84% when compared to the direct fine model optimization (correspondingly, 375 evaluations were required in the fine model optimization to reach this cost function value, cf. Figure 4).

Exploiting the improved scheme, a similarly accurate solution – both in terms of parameter match and optimal fit of the target data – can be obtained at a remarkably lower cost of only 17 equivalent fine model evaluations (point 3 in Figure 4). This is over three times less than for the original response correction scheme corresponding to a reduction of the total optimization cost of about 96%. Specific parameter values and model responses of this solution are omitted here, since they are similar to those of the original solution $\mathbf{u}_{s1}^*$.

Table 1. Solutions $\mathbf{u}_c^*$, $\mathbf{u}_f^*$, $\mathbf{u}_{s1}^*$ and $\mathbf{u}_{s2}^*$ of an illustrative coarse, fine model optimization and of a SBO run, exploiting the original and the improved correction scheme. Solutions $\mathbf{u}_{s1}^*$ and $\mathbf{u}_{s2}^*$ correspond to points 1 and 2 in Figure 4.

iterate	u_1	u_2	...									u_{12}
	SBO (original and improved scheme)											
$\mathbf{u}_{s1}^*$	0.705	0.626	0.044	0.015	0.060	0.937	1.908	0.016	0.147	0.020	0.629	4.237
$\mathbf{u}_{s2}^*$	0.738	0.604	0.028	0.010	0.036	1.024	1.678	0.010	0.206	0.020	0.541	4.318
	Coarse model optimization											
$\mathbf{u}_c^*$	0.300	1.066	0.036	0.065	0.064	0.025	0.040	0.065	0.010	0.012	0.730	3.448
	Fine model optimization											
$\mathbf{u}_f^*$	0.747	0.596	0.025	0.010	0.030	0.999	2.046	0.010	0.203	0.020	0.493	4.310
$\mathbf{u}_d$	0.750	0.600	0.025	0.010	0.030	1.000	2.000	0.010	0.205	0.020	0.500	4.320

On the other hand, when exploiting the improved correction scheme, a solution $\mathbf{u}_{s2}^*$ (point 2 in Figure 4) with a significantly higher accuracy – again both in terms of parameter match and optimal fit of the target data – can be obtained (cf. Figure 5 and Table 1) at the same cost as were required for the original one $\mathbf{u}_{s1}^*$, i.e., 60 equivalent fine model evaluations.

It should be emphasized that the surrogate model utilized in this work only satisfies zero-order consistency with the fine model. Still, as demonstrated in this section, the performance of our surrogate-based optimization process is satisfactory, particularly in terms of obtaining a good match between the model response and a given target output. Improved matching between the optimized model parameters and those corresponding to the target output could be obtained by executing larger number of SBO iterations (cf. Figure 4), which is mostly because of low sensitivity of the model with respect to some of the parameters. Also, the use of derivative information together with the trust-region convergence safeguards [4,8] would bring further improvement in terms of matching accuracy. Clearly, the trade-offs between the accuracy of the solution and the extra computational overhead related to sensitivity calculation has to be investigated. The aforementioned issues will be the subject of future research.

6 Conclusions

Parameter identification in climate models can be computationally very expensive or even beyond the capabilities of modern computer power. Before a transient simulation of a model (e.g., used for predictions) is possible, the latter has to be calibrated, i.e., relevant parameters have to be identified using measurement data. This is the point where large-scale optimization methods become crucial for a climate system forecast.

Using the high-fidelity (or fine) model under consideration in conventional optimization algorithms that require large number of model evaluations is often infeasible. Therefore, the development of faster methods that aim at reducing the optimization cost,

such as surrogate-based optimization (SBO) techniques, are highly desirable. The idea of SBO is to replace the high-fidelity model in the optimization run by a surrogate, its computationally cheap and yet reasonably accurate representation.

As a case study, we have investigated parameter optimization of a representative of the class of one-dimensional marine ecosystem models. As demonstrated in our previous work, a simple multiplicative response correction applied to a temporally coarser discretized physics-based low-fidelity (coarse) model of the system of interest is sufficient to create a reliable surrogate of the original, high-fidelity ecosystem model, which can be used as a prediction tool to calibrate the latter. This approach allowed us to yield remarkably good results, both in terms of the quality of the final solution and, most importantly, in terms of the relative reduction in the total optimization cost, about 84% when compared to the direct fine model optimization.

In this paper, we demonstrated that the correction scheme can be enhanced to alleviate the difficulties of its original version, which results in further improvement of the surrogate model accuracy and overall performance of the optimization algorithm utilizing this surrogate. The optimization cost was reduced by a factor of three (from 16% to 5% of the direct high-fidelity model optimization optimization cost), which corresponds to the cost savings of 95%.

Improvements of the present approach by utilizing additionally sensitivity information of the low- and the high-fidelity model in the alignment of the low-fidelity model as well as trust-region convergence safeguards applied to enhance the optimization process are expected to further improve the robustness of the algorithm and the accuracy of the solution. The trade-offs between the accuracy and extra costs due too sensitivity evaluation will have to be inspected.

Acknowledgements. The authors would like to thank Andreas Oschlies, IFM Geomar, Kiel. This research was supported by the DFG Cluster of Excellence Future Ocean.

References

1. Bandler, J.W., Cheng, Q.S., Dakroury, S.A., Mohamed, A.S., Bakr, M.H., Madsen, K., Søndergaard, J.: Space mapping: The state of the art. IEEE T. Microw. Theory 52(1) (2004)
2. Banks, H.T., Kunisch, K.: Estimation Techniques for Distributed Parameter Systems. Birkhäuser (1989)
3. Bucker, H.M., Fortmeier, O., Petera, M.: Solving a parameter estimation problem in a three-dimensional conical tube on a parallel and distributed software infrastructure. Journal of Computational Science 2(2), 95–104 (2011); Simulation Software for Supercomputers
4. Conn, A.R., Gould, N.I.M., Toint, P.L.: Trust-region methods. Society for Industrial and Applied Mathematics, Philadelphia (2000)
5. Fennel, W., Neumann, T.: Introduction to the Modelling of Marine Ecosystems. Elsevier (2004)
6. Forrester, A.I.J., Keane, A.J.: Recent advances in surrogate-based optimization. Prog. Aerosp. Sci. 45(1-3), 50–79 (2009)
7. Gill, A.E.: Atmosphere - Ocean Dynamics. International Geophysics Series, vol. 30. Academic Press (1982)
8. Koziel, S., Bandler, J.W., Cheng, Q.S.: Robust trust-region space-mapping algorithms for microwave design optimization. IEEE T. Microw. Theory 58(8), 2166–2174 (2010)

9. Leifsson, L., Koziel, S.: Multi-fidelity design optimization of transonic airfoils using physics-based surrogate modeling and shape-preserving response prediction. Journal of Computational Science 1(2), 98–106 (2010)
10. Majda, A.: Introduction to PDE's and Waves for the Atmosphere and Ocean. AMS (2003)
11. Marchuk, G.I.: Methods of Numerical Mathematics, 2nd edn. Springer (1982)
12. McGuffie, K., Henderson-Sellers, A.: A Climate Modelling Primer, 3rd edn. Wiley (2005)
13. Oschlies, A., Garcon, V.: An eddy-permitting coupled physical-biological model of the north atlantic. 1. sensitivity to advection numerics and mixed layer physics. Global Biogeochem. Cy. 13, 135–160 (1999)
14. Prieß, M., Koziel, S., Slawig, T.: Surrogate-based optimization of climate model parameters using response correction. Journal of Computational Science (2011) (in press)
15. Queipo, N.V., Haftka, R.T., Shyy, W., Goel, T., Vaidyanathan, R., Tucker, P.K.: Surrogate-based analysis and optimization. Prog. Aerosp. Sci. 41(1), 1–28 (2005)
16. Rückelt, J., Sauerland, V., Slawig, T., Srivastav, A., Ward, B., Patvardhan, C.: Parameter optimization and uncertainty analysis in a model of oceanic CO_2-uptake using a hybrid algorithm and algorithmic differentiation. Nonlinear Analysis B Real World Applications 10(1016), 3993–4009 (2010)
17. Sarmiento, J.L., Gruber, N.: Ocean Biogeochemical Dynamics. Princeton University Press (2006)
18. Simpson, T.W., Poplinski, J.D., Koch, P.N., Allen, J.K.: Metamodels for computer-based engineering design: Survey and recommendations. Eng. Comput. 17, 129–150 (2001), 10.1007/PL00007198
19. Smola, A.J., Schölkopf, B.: A tutorial on support vector regression. Stat. Comput. 14, 199–222 (2004), 10.1023/B:STCO.0000035301.49549.88
20. Søndergaard, J.: Optimization using surrogate models - by the space mapping technique. PhD thesis, Informatics and Mathematical Modelling, Technical University of Denmark, DTU, Richard Petersens Plads, Building 321, DK-2800 Kgs. Lyngby, Supervisor: Kaj Madsen (2003)
21. Tarantola, A.: Inverse Problem Theory and Methods for Model Parameter Estimation. SIAM (2005)